A&A 370, 974–981 (2001)
DOI: 10.1051/0004-6361:20010275

Astronomy & Astrophysics

The radial velocities of the RS CVn star UX Ari*,**

A triple system with a binary on the same line of sight

R. Duemmler[1] and V. Aarum[2,***]

[1] Astronomy Division, PO Box 3000, 90014 University of Oulu, Finland
[2] Institute of Theoretical Astrophysics, University of Oslo, PO Box 1029 Blindern, 0315 Oslo, Norway

Received 12 October 2000 / Accepted 15 February 2001

Abstract. UX Ari belongs to the class of very active RS CVn stars and has recently been the target of surface (Doppler) imaging. Although this technique needs a quite accurate determination of the orbit (in order to have the correct period for phasing and the correct Doppler shift correction of the line profiles) we found only one, quite old orbit solution, which has subsequently been used by everyone.
We used published radial velocities (RVs), supplemented by a large number (124) of our own recent, high-accuracy RVs of both the primary (K0 IV) and the secondary (G5 V) to improve the orbit of UX Ari. In addition to the improved set of parameters, we found that the γ velocity of the system is systematically changing over time. It seems that UX Ari is a triple system. Actually, a third star is weakly present in the spectrum. While its RV is also changing, it is not a member of the system, but happens to be on the same line of sight.
Finally, conclusions about the physical parameters of the objects from the orbits are presented.

Key words. stars: individual: UX Ari – stars: binaries: spectroscopic – stars: late-type – stars: activity – techniques: radial velocities

1. Introduction

UX Ari (HD 21242; K0 IV + G5 V) is a short-period ($P \approx 6\overset{\mathrm{d}}{.}4$), double-lined spectroscopic binary. It belongs to the class of RS CVn stars, i.e. at least the cool primary shows signs of activity. Thus, it is listed in the catalogue by Strassmeier et al. (1993), where more information on the system may be found (UX Ari = CABS 28); it was also put in our long term programme of surface imaging of active stars (for results see e.g. Berdyugina et al. 1998).

Surface imaging needs good orbital parameters. The spectral lines, whose distortions are followed through the rotational phases[1] need to have the Doppler shift due to the orbital motion removed; while experience shows that small residual shifts do not change the main surface structures, the extra noise in the data might lead to a lower quality of the map. Normally, the cross-correlation technique can be used to align spectra and remove radial velocity shifts without knowledge of any orbital parameters. However, cross-correlation relies on the assumption that the spectral features in the programme spectrum and the template are identical, which they are not in the case of active stars due to the distortions caused by spots. This leads to systematic radial velocity errors. It is hoped that if one compiles a large set of radial velocities spanning a long time, the constraints of orbital motion and the limited lifetime of spots allow the determination of a good set of orbital parameters despite the fact that individual radial velocities obtained in a short time span are systematically shifted. In order to calculate the rotational phases, a good value for the period needs to be known. This is especially important if maps obtained during several seasons are to be compared: an incorrect period and conjunction time lead to increasing phase shifts which mimic motions of the surface structure which are not real and lead to incorrect interpretation of the long term behaviour of the surface structures. Thus a (re-)determination of the orbit prior to surface imaging is strongly recommended.

For UX Ari, there seems to exist only one orbit determination: that by Carlos & Popper (1971). Given the age and the low number of measurements used, we felt it long overdue to compute a new orbit and improve the orbital

Send offprint requests to: R. Duemmler,
e-mail: Rudolf.Duemmler@Oulu.Fi

* Based on observations collected at the Nordic Optical Telescope (NOT), European Northern Observatory, La Palma, Spain, and at the McDonald and Kitt Peak Observatories, USA.

** Table 2 is only available in electronic form at the CDS via anonymous ftp to cdsarc.u-strasbg.fr (130.79.128.5) or via
http://cdsweb.u-strasbg.fr/cgi-bin/qcat?J/A+A/370/974

*** Visiting astronomer, Kitt Peak and McDonald observatories, USA.

[1] Given the evolved state of one of the components and the short period, it is reasonable to assume synchronized rotation, i.e. $P_{\mathrm{rot}} = P_{\mathrm{orb}}$.

Table 1. The wavelength resolution ($R = \lambda/\Delta\lambda$) and range in signal-to-noise ratios (S/N) at 6400 Å for each dataset

Set	R	S/N
S95	86 000	270–420
S96	71 000	280–390
M99	36 000	180–390
K99	86 000	90–170
M00	48 000	140–360

parameters as much as possible. The time difference between the first observation given by Carlos & Popper and our last observation is more than 42 years, which lets us hope to significantly improve the period and subsequently all other orbital parameters.

Another finding makes an accurate inspection of the orbit particularly interesting. Lestrade et al. (1999) performed high-precision VLBI astrometry of, among others, UX Ari. They used observations at 10 epochs between July 1983 and May 1994 to calculate the acceleration of UX Ari's position in the sky. The resulting acceleration was much larger than the perspective secular change in proper motion and could be caused by a third body. According to Lestrade et al. (1999), the orbital period of this system should be many times their 11-year VLBI data span.

2. Observations and data reductions

The new high-resolution, high signal-to-noise spectra were obtained for the purpose of surface imaging during five observing runs using three telescope-instrument combinations:

- 5 spectra obtained in December 1995 using the high-resolution échelle spectrograph SOFIN (Tuominen 1992) mounted at the Cassegrain focus of the 2.56 m Nordic Optical Telescope (NOT) on La Palma, Canary Islands, Spain (hereafter denoted S95);
- 10 spectra obtained in November/December 1996 using NOT/SOFIN (hereafter denoted S96);
- 64 spectra obtained in January 1999 using the Sandiford Cassegrain Échelle Spectrograph mounted on the 2.1 m Otto Struve Telescope at McDonald Observatory, Texas, USA (hereafter denoted M99);
- 23 spectra obtained in February 1999 using the Coudé CCD Spectrograph receiving light from the 0.9 m Coudé-Feed Telescope at Kitt Peak National Observatory, Arizona, USA (hereafter denoted K99);
- 22 spectra obtained in January 2000 again using the 2.1 m telescope with the Sandiford spectrograph at McDonald Observatory (hereafter denoted M00).

Table 1 shows the wavelength resolution ($\lambda/\Delta\lambda$) at 6400 Å and the range of signal-to-noise ratios at 6400 Å for each dataset. The spectrograph slit widths were chosen so that one resolution element (FWHM of the ThAr comparison lines) was 2–3 CCD-pixels. The spectra in K99 have considerably lower signal-to-noise ratios than the other datasets due to the smaller telescope.

Table 3. Measurements from speckle interferometry and from Hipparcos (ESA 1997) of the angular separation ϑ between the RS CVn system and the third star at different epochs (as Besselian year)

Epoch	ϑ ($''$)	Reference
1985.8431	0.432	McAlister et al. (1987)
1991.25	0.340	Hipparcos (ESA 1997)
1995.9237	0.297	Hartkopf et al. (1997)
1996.8658	0.256	Hartkopf et al. (2000)

The spectra in S95 and S96 were reduced using the 3A Software Package (Ilyin 1996). It uses two-dimensional dispersion curves (rows and columns of the CCD; see e.g. Duemmler et al. 1997 for a more thorough description) in order to calibrate the wavelength scale. The spectra in M99 were reduced using the 4A Software Package (Ilyin 2000). The spectra in K99 and M00 were reduced using IRAF. 4A and IRAF use three-dimensional dispersion curves (rows and columns of the CCD as well as time on the basis of several comparison spectra) to calibrate the wavelength scale. For all spectra, telluric lines based on the wavelengths given by Pierce & Breckinridge (1973) were used prior to heliocentric correction to establish the accurate wavelength zero point, correcting for tiny geometrical shifts between the comparison and stellar images due to bending of the spectrograph and the slit-effect, i.e. the shifts due to the fact that the optics is not homogeneously illuminated by the stellar light (Griffin & Griffin 1973; Ilyin 2000).

The projected equatorial rotational velocity $v \sin i$ of the subgiant primary in the RS CVn binary was determined from our measurements using a Fourier-transform technique described by Gray (1988; 1992, Chap. 17). The result is $v \sin i = 39\,\mathrm{km\,s^{-1}}$. For the secondary, a value of $v \sin i = 7.5\,\mathrm{km\,s^{-1}}$ was determined by comparing spun-up standard spectra with that of the secondary, a value consistent with the one given by Vogt & Hatzes (1991).

The radial velocities (RVs) were obtained by cross-correlating the UX Ari spectra with spectra of RV standard stars. For the primary we used spectra of β Gem (K0 IIIb, RV= $+(3.3 \pm 0.1)\,\mathrm{km\,s^{-1}}$) observed in the same run as the UX Ari spectra, reduced in the same way and artificially spun up to match $v \sin i$ of the primary. For the secondary we used the solar FTS spectrum (Kurucz et al. 1984), artificially spun up to match $v \sin i$ of the secondary. The RVs are weighted averages of the individual RVs measured in several orders. The measured RVs and their standard deviations are given in Table 2.

In the spectra of UX Ari there are also weak lines from a third star present. This star was first mentioned by McAlister et al. (1987) when they measured the angular separation between the RS CVn binary and the third star. This and other measurements of the angular separation are given in Table 3. From Table 3 it seems that the

angular separation has decreased by almost 0.″2 from 1985.8 to 1996.9. It is not known whether the third star is part of the UX Ari system or a star that just happens to lie on the same line of sight. Its spectral classification is also not known, although Fabricius & Makarov (2000) determined its B and V magnitudes based on Hipparcos (ESA 1997) data. Their B and V magnitudes yield $B-V=1.19\pm0.06$ for the third star. This in turn yields a spectral type of K5 if the star is unreddened and on the main sequence (Gray 1992). Vogt & Hatzes (1991) successfully used a synthetic G5 V spectrum to subtract the lines of the third star from the composite spectrum, and we used the solar FTS spectrum as RV template to measure the radial velocities of this star.

Before RV measurements of the third star could be carried out, however, the spectral flux contributions from the primary and the secondary had to be removed from the composite spectrum. Otherwise, the weak lines of the third star are too strongly influenced by the stronger lines of the other two components.

The spectral flux contribution from the primary (secondary) was removed using an observed spectrum of a single, inactive star of the same spectral classification as the primary (secondary). We used HD 71952 (K0 IV, $V=6.^{\rm m}25$) and HD 84453 (K0 IV, $V=6.^{\rm m}83$) for the primary and HD 23565 (G5 V, $V=7.^{\rm m}70$), HD 51419 (G5 V, $V=6.^{\rm m}94$) and HD 71148 (G5 V, $V=6.^{\rm m}30$) for the secondary. The single star was observed in the same run as UX Ari and reduced in the same way. Its spectrum was artificially spun up to match $v\sin i$ of the primary (secondary), scaled to match the relative continuum flux contribution of the primary (secondary) and shifted by cross-correlation to the position of the primary (secondary) in the composite spectrum. Finally, the spun-up, scaled and shifted spectrum of the single star was subtracted from the composite spectrum. The relative continuum flux contribution for each component was determined using the residual line strength in the composite spectrum.

The spectrum separation technique itself, as well as what applying it to our UX Ari observations can teach us about the three components in the UX Ari spectrum, will be described by Aarum & Engvold (in preparation). The results of applying the surface (Doppler) imaging technique to our UX Ari observations (and thus the details of the line profiles) will be described by Aarum et al. (in preparation).

3. The radial velocity curves of UX Ari

3.1. The data from the literature

A significant improvement of all orbital parameters depends strongly on the value of the period, which in turn is more sensitive to the overall time span covered by the measurements than to their quality. Thus, we supplement our new radial velocities with data from the literature to increase the time span.

There are not many RVs of UX Ari to be found. The oldest dataset is due to Carlos & Popper (1971). It contains a few RVs obtained in the 1950s, but mostly data from 1967 to 1970; the total number of RV pairs is 28. The second big dataset is due to Duquennoy et al. (1991), containing 36 timepoints with RVs (however often only for one of the two stars) obtained mostly in 1977; a few RVs are measured in 1985–1988. Duquennoy et al. (1991) give only the RVs; they do not determine or improve the orbital parameters. Another dataset is given by Heintz (1981). There are only 3 RVs for each component given, and, when compared to a preliminary orbit, they have considerable scatter. This would give them such a low weight in the combined dataset that, together with their small number and the fact that their observing times overlap with the dataset of Duquennoy et al. (1991), we decided not to use them at all.

3.2. The weights

The optimal weights in a least squares fit are the inverse variances of the individual measurements. For all datasets, individual error estimates for the RVs are known, except for the set given by Carlos & Popper (1971). Thus, we decided to use the inverse variance as the weight, and determine an estimate for this for the Carlos & Popper set.

An independent orbital fit of a double-lined binary RV curve to the data of Carlos & Popper (1971) alone was performed, using their relative weights[2]. The resulting orbital parameters are close to those given by Carlos & Popper. Standard deviations for measurements having unit weight for the primary ($1.6\,\mathrm{km\,s^{-1}}$) and the secondary ($1.9\,\mathrm{km\,s^{-1}}$) were obtained and used to calculate for each measurement an error by combining them with the relative weight. These are the errors given in Table 2 for the measurements of Carlos & Popper (1971) and used to calculate the weights as the inverse variances.

All other measurements obtained their weights as the inverse variances based on the errors as published. Preliminary orbit fits, however, indicated that a considerable improvement is achieved when ignoring all measurements obtained from blended lines, i.e. with RV-differences $<40\,\mathrm{km\,s^{-1}}$ between primary and secondary. Therefore, we decided to give all those measurements weight 0 in the following; they are indicated by negative errors in Table 2.

During the first orbital fits it turned out that χ^2 for the primary is significantly larger than χ^2 for the secondary, although the smaller accuracy of the RVs due to the much broader lines is already reflected by the much larger RV-errors. This could be due to the systematic deviations of the RVs caused by the fine-structure of the line profiles because of the spot activity. We therefore multiplied all

[2] except for the 3 very old measurements, which had weights 0 in their final fit, but obtained 0.7 here; finally, since it improved the fit significantly, all data with RV-differences $<40\,\mathrm{km\,s^{-1}}$ between primary and secondary obtained weights 0.

weights of the primary by an additional factor 0.65 to equalize χ^2 for the primary and the secondary.

3.3. The first fit results: γ is changing

For each dataset, i.e. Carlos & Popper (1971), Duquennoy et al. (1991), and each of the seasons of our own observations, an individual orbital fit has been done. By this we established:

- that there is no significant (as compared to the formal fit errors) change of any orbital parameter
- *except* the velocity γ of the centre of mass of the system, which is different for each dataset.

The following fit, combining all datasets, thus requires that all orbital parameters are the same, but allows each dataset to obtain its own velocity zero-point, i.e. its own γ velocity. The results of this fit are given in Table 4 and compared to the orbital parameters given by Carlos & Popper (1971). Here, and throughout the paper, errors are formal fit errors, obtained from the curvature of the χ^2 hypersurface or from error progression, and are likely underestimates of the true errors.

The results can be summarized as follows:

- Most orbital parameters given by Carlos & Popper (1971) have been confirmed.
- Due to the much larger database and the higher accuracy of the later data, the accuracy of the orbital parameters has considerably increased. The period, in particular, is shorter than that given by Carlos & Popper, while still being consistent with it because of their larger error.
- Despite the high significance given to the eccentricity, we do not believe that the orbit is really elliptical. Firstly, the eccentricity is very small; secondly, its error is relatively large, so that the eccentricity is just a 2.5σ detection. Thirdly, as will be seen later, there are systematic effects in the radial velocity curve which might mimic the effects of a (small) non-zero eccentricity. Finally, the deviations from the circular orbit are so negligible that all other orbital parameters are indistinguishable from those obtained for the circular orbit; thus, no harm is done by neglecting e in the following even if it should be real.
- The values of the velocity of the centre of mass γ of the system are clearly inconsistent with each other and need further consideration.

While it is not uncommon to have different velocity zero-points from different instruments, especially when old data are involved, the situation here is different. Firstly, there are two pairs of datasets (S95, S96 and M99, M00) which were taken by the same instruments, however one year apart. The γ velocities are inconsistent within the groups which only becomes apparent thanks to the high quality and number of the radial velocities leading to really small errors in γ. Secondly, all new data are reduced in the same way. This means in particular that the wavelength scale for each spectrum is adjusted (prior to heliocentric correction) to the same wavelength system established by a large number of telluric atmospheric lines based on the wavelengths given by Pierce & Breckinridge (1973). This technique should remove all effects caused by the slit-effect and temporal effects like those caused by the change of ambient temperature and pressure and (for the Cassegrain-spectrographs) bending of the spectrograph due to motion of the telescope. Furthermore, all RVs were measured using the same star as template (the IAU RV-standard β Gem for the primary and the solar FTS-spectrum for the secondary; while β Gem has been observed during the same runs with the same instruments as UX Ari, and reduced in the same way, the solar FTS-spectrum used is always the same). Additionally, the paper by Duquennoy et al. (1991) states that their radial velocities are on the IAU faint ($m_V \geq 4.3$) standard system; yet the difference between γ_{DMH} and γ_{S96} is 8.4σ. On the other hand, the difference between γ_{M99} and γ_{K99}, which were obtained with different instruments a month apart, is only 1.5σ. The difference between γ_{S96} and γ_{M00} is 44σ! Finally, it seems that we have, at least for the new data, a systematic behaviour of γ: it seems to increase from 1995 to 1996, and from then on it systematically decreases with time.

For these reasons, we believe that the variation in γ is genuine and not caused by any instrumental effect. The short-period RS CVn system UX Ari is obviously in an accelerated motion, most likely around the centre of mass with a third star.

3.4. The final fit of the inner orbit

If we accept this interpretation, we have to make two changes in order to obtain the final orbital parameters: First, the old datasets from the literature cover several years, and we see from the large difference (as compared to the error) between 1999 and 2000 that γ is changing much over one year; we thus have to subdivide all datasets so that each subset does not cover more than 1 year. Secondly, if γ is changing, so is the factor between the period in the observer's frame and the period in the restframe of the system. Given that there is no evidence for any change of the orbital parameters, except γ, we can assume that the period in the restframe of the system is constant, but not the one in the observer's frame.

The final orbital fit is thus a weighted fit (using the same weights as before) to 17 subsets, ensuring that all parameters have the same values for all datasets, except γ. Given the small eccentricity found before, this fit is forced to be circular. The subsets have been identified in Table 2. The resulting orbit is given in Table 5 and shown in Fig. 1. Unfortunately, several of the 17 datasets consist of only 1–3 measurements, so determination of γ is only possible, because no other parameter is determined for these small datasets alone; nevertheless, for these small datasets and for others due to large errors in the measurements, the

Table 4. Two orbital solutions using the data and errors given in Table 2; the weights of the primary have been additionally reduced by a factor 0.65. Fit 1: circular, 7 different γ velocities allowed; the index of γ identifies the dataset, where CP stands for Carlos & Popper (1971) and DMH for Duquennoy et al. (1991). Fit 2: like Fit 1, but allowing for $e > 0$. C&P: parameters of Carlos & Popper (1971)

parameter	Fit 1	Fit 2	C&P [1]
$P_{\rm obs}$ (days)	6.4378553 ± 0.0000046	6.4378564 ± 0.0000046	6.43791 ± 0.00008
K_1 ($\mathrm{km\,s^{-1}}$)	57.88 ± 0.17	57.93 ± 0.17	59.4 ± 0.6
K_2 ($\mathrm{km\,s^{-1}}$)	66.978 ± 0.033	66.971 ± 0.033	66.7 ± 0.8
e	0.0 (fixed)	0.0018 ± 0.0007 [2]	0.0 (fixed)
ω (deg)	—	31.7 ± 20.0	—
T_0 (HJD) [3]	$2450642.00075 \pm 0.00077$	2450642.57 ± 0.36	—
$T_{\rm conj}$ (HJD) [4]	$2450640.39129 \pm 0.00077$	2450640.39 ± 0.51	2450640.44 ± 0.13 [5]
$a_1 \sin i$ ($R_\odot$)	7.362 ± 0.021	7.368 ± 0.021	7.55 ± 0.13 [6]
$a_2 \sin i$ ($R_\odot$)	8.5192 ± 0.0042	8.5183 ± 0.0042	8.50 ± 0.13 [6]
$m_1 \sin^3 i$ ($M_\odot$)	0.6964 ± 0.0066	0.6968 ± 0.0066	0.71 ± 0.01
$m_2 \sin^3 i$ ($M_\odot$)	0.6018 ± 0.0055	0.6027 ± 0.0054	0.63 ± 0.01
$\gamma_{\rm CP}$ ($\mathrm{km\,s^{-1}}$)	26.46 ± 0.75	26.47 ± 0.74	26.5 ± 0.6
$\gamma_{\rm DMH}$ ($\mathrm{km\,s^{-1}}$)	27.30 ± 0.23	27.29 ± 0.23	—
$\gamma_{\rm S95}$ ($\mathrm{km\,s^{-1}}$)	28.806 ± 0.047	28.911 ± 0.061	—
$\gamma_{\rm S96}$ ($\mathrm{km\,s^{-1}}$)	29.273 ± 0.049	29.309 ± 0.053	—
$\gamma_{\rm M99}$ ($\mathrm{km\,s^{-1}}$)	28.043 ± 0.067	28.094 ± 0.070	—
$\gamma_{\rm K99}$ ($\mathrm{km\,s^{-1}}$)	27.898 ± 0.066	27.945 ± 0.071	—
$\gamma_{\rm M00}$ ($\mathrm{km\,s^{-1}}$)	25.905 ± 0.058	25.921 ± 0.061	—
σ ($\mathrm{km\,s^{-1}}$) [7]	1.82, 0.25	1.79, 0.25	—

[1] Note, that Carlos & Popper (1971) give mean errors, which have been converted to standard deviations here for consistency.
[2] A Lucy-Sweeney F-test (Lucy & Sweeney 1971; Lucy 1989) gives a 97.7% significance for this eccentricity.
[3] For $e = 0$, HJD of maximum RV of the primary, for $e > 0$ that of periastron passage.
[4] HJD of the conjugation with the secondary (hotter star) in the back.
[5] computed from their value ("earlier star") and their period with error propagation.
[6] computed from their $a \sin i$ and their mass-ratio, retaining their error for $a \sin i$.
[7] standard deviation of a single RV of mean weight, separately for primary and secondary, respectively.

error of γ is sometimes so large that it hides any change of γ. Due to this and due to the timing of the older observations, no indication for a changing γ could be detected before our new, accurate datasets.

In Fig. 1 we see that there is a nearly perfect fit of the RVs of the secondary. For the primary, however, we notice a large, systematic deviation near RV-maximum: Most new measurements deviate from the curve towards larger velocities. No such deviations are seen near the minimum. This is the reason for the larger χ^2 of the primary as compared to the secondary mentioned above which motivated us to introduce the extra weight reduction factor of 0.65 for the RVs of the primary. It will be very interesting to see the surface maps of the primary (Aarum et al., in preparation): when the primary is moving away from us, there should be a strong surface feature in the facing hemisphere that lets us overestimate the RV, which is not visible, when the star shows us the other hemisphere. Also, since the deviation is in nearly all new measurements (which cover more than 4 years), this feature must be very long-lived. It cannot be a hot spot in the sub-secondary point, because this would also be visible at RV-minimum.

This also shows that it would not be appropriate to use cross-correlation techniques to adjust the spectra for surface imaging: if we would have chosen a spectrum near RV-maximum as template and adjusted all other spectra to it, we would have introduced a significant wavelength shift. It is thus essential that the Doppler shift corrections prior to surface imaging come from an accurate orbit, determined over a long time span.

3.5. The preliminary outer orbit

Now that the γ velocities at 17 timepoints are known, we could try to determine the parameters of the outer orbit. Unfortunately, this is not simple. While the new data show beyond any doubt that γ is changing, they alone do not allow to determine the orbit. A maximum γ was observed in 1996, but since then γ has been decreasing steadily; no minimum has been observed yet. That means that from the new data alone, only lower limits for the period $P_{\rm out}$ of the outer orbit and the RV-amplitude $K_{\rm out}$ can be obtained. The old datasets, due to their unfortunate timings and their large errors do not improve this situation

Table 5. The final orbital solution ($e = 0$) using the data and errors given in Table 2 split into 17 datasets; the weights are as before. The period used is always the period in the restframe of the system. All parameters are the same for all datasets, except γ. The weighted average HJD for each dataset (–2400000) is given together with the fitted γ

parameter		
$P_{\rm rest}$ (days)	6.4372703 ± 0.0000069	
K_1 ($\mathrm{km\,s^{-1}}$)	57.86 ± 0.17	
K_2 ($\mathrm{km\,s^{-1}}$)	66.980 ± 0.036	
T_0 (HJD)	$2450642.00204 \pm 0.00081$	
$T_{\rm conj}$ (HJD) [1]	$2450640.39272 \pm 0.00081$	
$a_1 \sin i$ ($R_\odot$)	7.358 ± 0.022	
$a_2 \sin i$ ($R_\odot$)	8.5186 ± 0.0045	
$m_1 \sin^3 i$ ($M_\odot$)	0.6962 ± 0.0069	
$m_2 \sin^3 i$ ($M_\odot$)	0.6013 ± 0.0056	
$\gamma_{\rm CP_1}$ ($\mathrm{km\,s^{-1}}$)	27.6 ± 4.0	34785.6460
$\gamma_{\rm CP_2}$ ($\mathrm{km\,s^{-1}}$)	28.8 ± 1.9	35001.9260
$\gamma_{\rm CP_3}$ ($\mathrm{km\,s^{-1}}$)	27.61 ± 0.97	39813.4043
$\gamma_{\rm CP_4}$ ($\mathrm{km\,s^{-1}}$)	26.4 ± 2.9	39926.6130
$\gamma_{\rm CP_5}$ ($\mathrm{km\,s^{-1}}$)	28.3 ± 1.1	40125.7212
$\gamma_{\rm CP_6}$ ($\mathrm{km\,s^{-1}}$)	28.1 ± 1.4	40519.1555
$\gamma_{\rm CP_7}$ ($\mathrm{km\,s^{-1}}$)	27.5 ± 1.1	40878.2310
$\gamma_{\rm DMH_1}$ ($\mathrm{km\,s^{-1}}$)	27.28 ± 0.23	43440.9205
$\gamma_{\rm DMH_2}$ ($\mathrm{km\,s^{-1}}$)	26.86 ± 0.58	46425.6050
$\gamma_{\rm DMH_3}$ ($\mathrm{km\,s^{-1}}$)	27.67 ± 0.76	46713.0793
$\gamma_{\rm DMH_4}$ ($\mathrm{km\,s^{-1}}$)	26.77 ± 0.94	46845.1837
$\gamma_{\rm DMH_5}$ ($\mathrm{km\,s^{-1}}$)	26.62 ± 0.51	47520.6140
$\gamma_{\rm S95}$ ($\mathrm{km\,s^{-1}}$)	28.806 ± 0.049	50055.6248
$\gamma_{\rm S96}$ ($\mathrm{km\,s^{-1}}$)	29.277 ± 0.052	50415.4416
$\gamma_{\rm M99}$ ($\mathrm{km\,s^{-1}}$)	28.026 ± 0.071	51186.5754
$\gamma_{\rm K99}$ ($\mathrm{km\,s^{-1}}$)	27.850 ± 0.067	51215.5638
$\gamma_{\rm M00}$ ($\mathrm{km\,s^{-1}}$)	25.877 ± 0.062	51559.1661
σ ($\mathrm{km\,s^{-1}}$) [2]	1.93, 0.26	

[1] HJD of the conjugation with the secondary in the back.
[2] standard deviation of a single RV of mean weight, separately for primary and secondary, respectively.

Table 6. The preliminary orbital solutions to $\gamma(t)$ using the γ values and average HJDs given in Table 5. The period $P_{\rm out}$ is given in the observer's frame

parameter	circular	elliptical
$P_{\rm out}$ (days)	3894 ± 66	7838 ± 23
$K_{\rm out}$ ($\mathrm{km\,s^{-1}}$)	2.90 ± 0.30	2.036 ± 0.061
e	0.0 (fixed)	0.622 ± 0.040
ω (deg.)	—	71.7 ± 3.6
T_0 (HJD)	2450495 ± 35	2451164 ± 24
$a_{\rm out} \sin i$ ($R_\odot$)	223 ± 23	247 ± 13
$f(m)$ ($M_\odot$)	0.0098 ± 0.0031	0.00329 ± 0.00050
$\gamma_{\rm out}$ ($\mathrm{km\,s^{-1}}$)	26.53 ± 0.22	27.23 ± 0.12
σ ($\mathrm{km\,s^{-1}}$)	0.30	0.073

much. This is with the exception of $\gamma_{\rm DHM_1}$ whose error is only $0.23\,\mathrm{km\,s^{-1}}$, and which will have a large impact on $P_{\rm out}$ and by that also allow an estimate of $K_{\rm out}$. However, any orbital fit to the γ velocities as they are available now has to be considered preliminary.

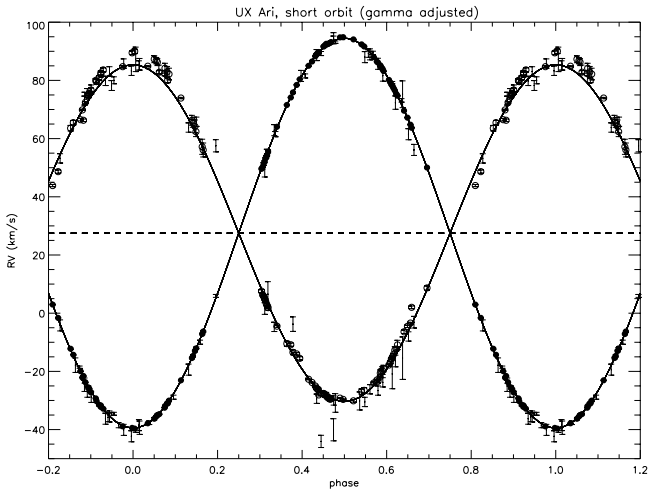

Fig. 1. Final orbit fit (as given in Table 5) showing as pure errorbars the measurements from the literature; our new measurements are shown with filled circles for the secondary (the errorbars are usually smaller than the symbol size) and as open circles for the primary. The different γ velocities have been shifted to a common value ($\gamma_{\rm DMH_1}$)

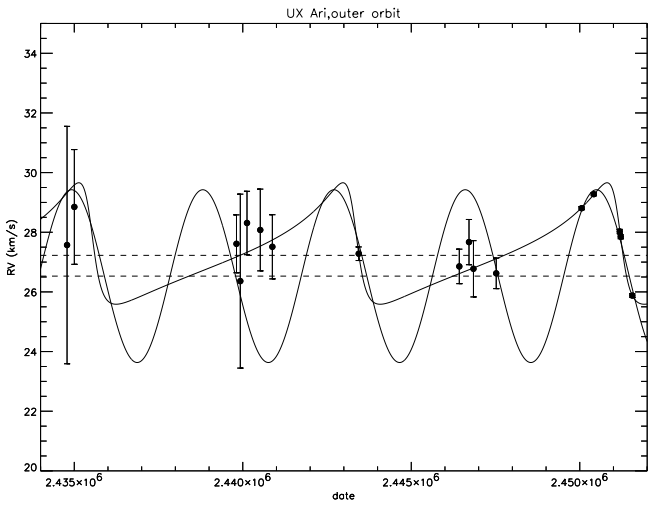

Fig. 2. The preliminary orbital fits to the 17 γ velocities given in Table 5. For our new data, the last 5 points, the errorbars are smaller than the symbol sizes

We have done a period search in the interval $P_{\rm out} = 4, ..., 46$ years. Two runs were performed, one fixing $e = 0$, the other allowing for an elliptical orbit. The results of both searches are given in Table 6; of all the orbit fits performed, the one yielding the smallest σ is given. While the elliptical orbit is *much* better than the circular one, given the small number of points and their large errors we cannot claim it to be correct.

The period of the circular orbit corresponds to $(10.66 \pm 0.18)\,\mathrm{yr}$ and the projected major axis $a_{\rm out} \sin i$ to $(1.04 \pm 0.11)\,\mathrm{AU}$; the period of the elliptical orbit is $(21.46 \pm 0.06)\,\mathrm{yr}$ and its projected major axis is $(1.15 \pm 0.06)\,\mathrm{AU}$.

Table 7. The radial velocities of the third star in the spectrum of UX Ari. The velocities are weighted averages of all RVs obtained during the corresponding run. The velocity from Vogt & Hatzes (1991, VH86/7), referring to the time Nov. 1986 to Jan. 1987, is also given; the velocity is inferred from their description and the assumption that they used the γ velocity of Carlos & Popper (1971); no error is available for their RV

dataset	RV_3 ($km\,s^{-1}$)
VH86/7	19.9
S95	14.76 ± 0.25
S96	15.532 ± 0.086
M99	19.483 ± 0.071
K99	19.917 ± 0.093
M00	23.43 ± 0.42

3.6. The third star

As already mentioned in Sect. 2, in the spectrum of UX Ari there are weak lines of a third star. Vogt & Hatzes (1991) measured its RV "stationary at $6.6\,km\,s^{-1}$ blueward of the γ velocity of the system". This statement refers to the time November 1986 to January 1987. Assuming that they used the γ velocity given by Carlos & Popper (1971), this velocity corresponds to $19.9\,km\,s^{-1}$. We also measured the velocities of the third star in the spectrum of UX Ari after subtracting the spectra of the primary and the secondary. We did not find any variation within a run; thus, we give the average velocities and standard deviations in Table 7.

It is clear that the velocity of the third star is also changing. However, there are several reasons to believe that the third star is not the body responsible for the changes of the γ velocity of the short-period RS CVn system:

- While the increase of RV_3 reflects the decrease of γ, γ reaches its maximum in 1996, while RV_3 reaches its minimum in (or before) 1995.
- In 1986/7 and 1999, the third star had similar RVs. Either its γ is less than the 26.5 or $27.2\,km\,s^{-1}$ obtained from the long-period orbit of UX Ari, or its period is at least 24 years (it must be longer, if 19.9 is below the γ velocity of that binary), more than 2 times longer than our estimate for the circular long-period orbit of UX Ari and still longer than the 21.5 yr estimated for the elliptical orbit. However, we caution that it is always possible that a crossing of $19.9\,km\,s^{-1}$ between 1986/7 and 1995 has been missed.
- Yet another confirmation is obtained from the conclusions presented in Sect. 4.

4. Conclusions

By using high-accuracy radial velocities of the double-lined RS CVn system UX Ari we have shown that the γ velocity is systematically changing; all other orbital parameters seem to be constant over time. Preliminary (circular and elliptical) orbital solutions of $\gamma(t)$ lead to a period of roughly 10 and 21 years, respectively. New, high-accuracy orbits of UX Ari are urgently needed to establish the accurate period of the long-period orbit.

It is interesting that our findings do not compare well with those of Lestrade et al. (1999). Their angular accelerations measured for UX Ari, if interpreted as consequences of the gravitational pull due to a third star, require a period of the outer orbit of many times their 11-year observational time span. Our circular orbit has a period even shorter than 11 yr; the eccentric orbit's period is less than twice 11 yr. Furthermore, their observations obtained during JD $\approx$ 2445000–2449000 covered, according to our eccentric orbit fit, the passage through the apastron, i.e. they should have noticed a change of direction in the proper motions. Our γs are only compatible with a much larger period if the eccentricity is even higher than $e \approx 0.6$. Our data time span is not long enough to allow for such a fit. Also for this reason new, high-quality γ measurements are of great importance.

Several arguments (see also below) indicate that the third star, which produces a weak third set of lines in the spectrum of UX Ari, is not the body responsible for the γ variations; but we found that the third star's RV is also systematically varying. Thus, UX Ari is (at least) a triple system with a single-lined spectroscopic binary on the same line of sight. Also for the third star further observations are needed to establish its orbit and to find out whether it is in the fore- or in the background.

If we take the preliminary long-period orbital solution seriously, the period in the observer's frame is changing between $6\overset{d}{.}437778$ and $6\overset{d}{.}437902$ with an error of $0\overset{d}{.}000011$[3]; thus, the period variation is highly significant (11σ). Nevertheless, the phase shift caused by this variation is negligible for Doppler imaging: the apparent motion of a really stationary surface feature during the 5.3 yr between maximum and minimum is only 2°. The systematic change of the radial velocity by almost $6\,km\,s^{-1}$, however, is highly significant and may lead to artifacts in the maps.

In the following, we want to draw some more conclusions about the physical parameters of the components in UX Ari:

- The spectral type of the secondary is given as G5 V (Vogt & Hatzes 1991), which is consistent with the results from our subtraction technique. If it were of significantly different spectral class, the subtraction of G5 V standards would lead to significant residuals in the subtracted spectrum. The classification of G5 V implies a mass of the secondary $m_2 = (0.95 \pm 0.05)\,M_\odot$. This value is obtained as an average between the values given by Schmidt-Kaler (1982) and Gray (1992, App. B); the error accounts for the difference between their values as well as a small classification error.
- Together with $m_2 \sin^3 i$ from Table 5 this yields an inclination of $i = 59\overset{\circ}{.}2 \pm 3\overset{\circ}{.}3$. This high inclination

[3] These numbers refer to the larger γ variations of the circular orbit (see Fig. 2).

(if the orbital and rotational axes are aligned) makes UX Ari an ideal target for surface imaging (for results see Aarum et al. 1999; Aarum et al., in preparation).

- i and $m_1 \sin^3 i$ (Table 5) give a mass of the primary of $m_1 = (1.100 \pm 0.060)\, M_\odot$.
- With m_1, m_2 and the mass functions $f(m)$ from the outer orbit (Table 6), and assuming that the inclination of the long-period orbit is also 59°.2, we get for the mass of the third body in the system $m = (0.460 \pm 0.052)\, M_\odot$ (for $e = 0$) and $m = (0.307 \pm 0.020)\, M_\odot$ (for $e \approx 0.6$). The larger of these masses corresponds to an early M star, whose M_V is at least 4^m fainter than that of the G5 secondary, much too faint to be responsible for the third set of lines visible in the spectrum of UX Ari, thus confirming our earlier conclusion that the third star in the spectrum is a binary accidentally on the same line of sight.
- The same conclusion is reached in another way: If the third star in the spectrum would be the body responsible for the γ variations, the amplitude of its RV curve would be $K_3 \geq 26.5 - 14.8 = 11.7\,\mathrm{km\,s^{-1}}$. This leads to a mass ratio of $m_3/(m_1 + m_2) = K_{\rm out}/K_3 \leq 0.25$ and with the above masses m_1, m_2 to $m_3 \leq 0.51\, M_\odot$, again an early M star with too small luminosity to account for the third set of lines.
- With the plausible assumption that the rotation of the two stars in the short-period system of UX Ari is synchronized with the orbit, i.e. $P_{\rm rot} = P_{\rm orb} = P_{\rm rest}$ and $i_{\rm rot} = i_{\rm orb}$, $v \sin i$ gives for the radii of the stars $R_1 = (5.78 \pm 0.13)\, R_\odot$, $R_2 = (1.11 \pm 0.08)\, R_\odot$. The radius of the primary is consistent with its subgiant classification; the radius of the secondary, however, is significantly larger than that of a G5 V star: Gray (1992, App. B) gives $0.96\, R_\odot$, while Schmidt-Kaler (1982) gives $0.92\, R_\odot$. With such a large radius the star should have spectral type G0–1 V according to both authors. This seems to be a large deviation for the classification; maybe, also this star has already expanded a little away from the main sequence.
- With the masses and radii we obtain for the surface gravities $\log g_1 = 2.96 \pm 0.03$, $\log g_2 = 4.32 \pm 0.07$. This means that the model spectra for the primary used in surface imaging can well be calculated with $\log g = 3$; no interpolation between the models, given by Kurucz (1993) in steps of $\Delta \log g = 0.5$, will be necessary.
- Given the inclination, we can compute $a = a_1 + a_2$, and from that and the mass ratio (Table 5) obtain the effective radii of the Roche-lobes (Eggleton 1983), i.e. the radii of the spheres having the same volumes as the Roche-lobes. We get $R_{\rm Rl,1} = 7.24 \pm 0.13$, $R_{\rm Rl,2} = 6.77 \pm 0.12$ (the errors neglect the (at most) 1% error of the Eggleton (1983) approximation).
- If we compare the Roche-lobe radii with the radii of the stars themselves it is clear that neither of the stars fills its Roche-lobe. However, the primary is close; a K0 giant has typically a radius of $11\, R_\odot$ (Gray 1992) and since the star will go on cooling, the final radius should be even larger. Thus, the RS CVn system of UX Ari will soon become a semi-detached binary.

Acknowledgements. The authors would like to thank the anonymous referee for his careful reading of the paper and his comments, which helped to significantly improve the paper. This work made use of the SIMBAD database, maintained at the CDS, Strasbourg, France. Part of this work is supported by the Norwegian Research Council under project number 122520/431.

References

Aarum, V., Berdyugina, S., & Ilyin, I. 1999, in Astrophysics with the NOT, Proc. Conf., Turku, August 12–15, 1998, ed. H. Karttunen, & V. Piirola, Univ. Turku, 222
Berdyugina, S. V., Berdyugin, A. V., Ilyin, I., & Tuominen, I. 1998, A&A, 340, 437
Carlos, R. C., & Popper, D. M. 1971, PASP, 83, 504
Duemmler, R., Ilyin, I. V., & Tuominen, I. 1997, A&AS, 123, 209
Duquennoy, A., Mayor, M., & Halbwachs, J.-L. 1991, A&AS, 88, 281
Eggleton, P. P. 1983, ApJ, 268, 368
ESA, 1997, The Hipparcos and Tycho catalogues, vols. 1–17, ESA–SP–1200
Fabricius, C., & Makarov, V. V. 2000, A&A, 356, 141
Gray, D. F. 1988, Lectures on Spectral-Line Analysis: F, G and K stars, The Publisher, Arva, Ontario
Gray, D. F. 1992, The Observation and Analysis of Stellar Photospheres (Cambridge University Press)
Griffin, R., & Griffin, R. 1973, MNRAS, 162, 243
Hartkopf, W. I., McAlister, H. A., Mason, B. D., et al. 1997, AJ, 114, 1639
Hartkopf, W. I., Mason, B. D., McAlister, H. A., et al. 2000, AJ, 119, 3084
Heintz, W. D. 1981, ApJS, 46, 247
Ilyin, I. V. 1996, Acquisition, Archiving and Analysis (3A) Software Package – User's Manual, Observatory, University of Helsinki
Ilyin, I. V. 2000, High resolution SOFIN CCD échelle spectroscopy, Ph.D. Thesis, University of Oulu, Finland
Kurucz, R. L. 1993, CD No. 13
Kurucz, R. L., Furenlid, I., Brault, J., & Testerman, L. 1984, Solar Flux Atlas from 296 to 1300 nm, National Solar Observatory Atlas No. 1
Lestrade, J.-F., Preston, R. A., Jones, D. L., et al. 1999, A&A, 344, 1014
Lucy, L. B. 1989, Obs. 109, No. 1090, 100
Lucy, L. B., & Sweeney, M. A. 1971, AJ, 76, 544
McAlister, H. A., Hartkopf, W. I., & Hutter, D. J. 1987, AJ, 93, 688
Pierce, A. K., & Breckinridge, J. B. 1973, Kitt Peak Contr. 559 (and addendum 1974)
Schmidt-Kaler, Th. 1982, in Landolt-Börnstein, Numerical Data and Functional Relationships in Science and Technology, New Series, Group VI: Astronomy, Astrophysics and Space Research (Springer, Berlin), vol. 2b, p. 30, Table 21
Strassmeier, K. G., Hall, D. S., Fekel, F. C., & Scheck, M. 1993, A&AS, 100, 173
Tuominen, I. 1992, NOT News, 5, 15
Vogt, S. S., & Hatzes, A. P. 1991, in The Sun and Cool Stars: activity, magnetism, dynamos, Proc. IAU Coll. 130, ed. I. Tuominen, D. Moss, & G. Rüdiger (Springer, Berlin), 297